

ANL/RE/CP-93201  
CONF-96/202--

M97053027

**SALT-OCCLUDED ZEOLITE WASTE FORMS:  
CRYSTAL STRUCTURES AND TRANSFORMABILITY**

J. W. RICHARDSON, JR.

Intense Pulsed Neutron Source Division, Argonne National Laboratory, Argonne, IL 60439 USA

RECEIVED  
MAY 27 1997  
OSTI

The submitted manuscript has been authored by a contractor of the U. S. Government under contract W-31-109-ENG-38. Accordingly, the U. S. Government retains a nonexclusive, royalty-free license to publish or reproduce the published form of this contribution, or allow others to do so, for U. S. Government purposes.

Describing work presented at the  
Materials Research Society Meeting  
Dec. 2-6, 1996 Boston, MS

Proceedings to be published in *Mat. Res. Soc. Symp. Proc.*

\*Work supported by U. S. Department of Energy, BES, contract No. W-31-109-ENG-38

DISTRIBUTION OF THIS DOCUMENT IS UNLIMITED

MASTER

The submitted manuscript has been authored by a contractor of the U. S. Government under contract No. W-31-109-ENG-38. Accordingly, the U. S. Government retains a nonexclusive, royalty-free license to publish or reproduce the published form of this contribution, or allow others to do so, for U. S. Government purposes.

## **DISCLAIMER**

**This report was prepared as an account of work sponsored by an agency of the United States Government. Neither the United States Government nor any agency thereof, nor any of their employees, make any warranty, express or implied, or assumes any legal liability or responsibility for the accuracy, completeness, or usefulness of any information, apparatus, product, or process disclosed, or represents that its use would not infringe privately owned rights. Reference herein to any specific commercial product, process, or service by trade name, trademark, manufacturer, or otherwise does not necessarily constitute or imply its endorsement, recommendation, or favoring by the United States Government or any agency thereof. The views and opinions of authors expressed herein do not necessarily state or reflect those of the United States Government or any agency thereof.**

**DISCLAIMER**

**Portions of this document may be illegible  
in electronic image products. Images are  
produced from the best available original  
document.**

# SALT-OCCLUDED ZEOLITE WASTE FORMS: CRYSTAL STRUCTURES AND TRANSFORMABILITY

J. W. RICHARDSON, JR.

Intense Pulsed Neutron Source Division, Argonne National Laboratory, Argonne, IL 60439 USA

## ABSTRACT

Neutron diffraction studies of salt-occluded zeolite and zeolite/glass composite samples, simulating nuclear waste forms loaded with fission products, have revealed complex structures, with cations assuming the dual roles of charge compensation and occlusion (cluster formation). These clusters roughly fill the 6-8 Å diameter pores of the zeolites. Samples are prepared by equilibrating zeolite-A with complex molten Li, K, Cs, Sr, Ba, Y chloride salts, with compositions representative of anticipated waste systems. Samples prepared using zeolite 4A (which contains exclusively sodium cations) as starting material are observed to transform to sodalite, a denser aluminosilicate framework structure, while those prepared using zeolite 5A (sodium and calcium ions) more readily retain the zeolite-A structure. Because the sodalite framework pores are much smaller than those of zeolite-A, clusters are smaller and more rigorously confined, with a correspondingly lower capacity for waste containment. Details of the sodalite structures resulting from transformation of zeolite-A depend upon the precise composition of the original mixture. The enhanced resistance of salt-occluded zeolites prepared from zeolite 5A to sodalite transformation is thought to be related to differences in the complex chloride clusters present in these zeolite mixtures. Data relating processing conditions to resulting zeolite composition and structure can be used in the selection of processing parameters which lead to optimal waste forms.

## INTRODUCTION

This work is carried out in support of a ceramic waste form development project at Argonne National Laboratory for salt waste generated from electrometallurgically conditioned spent nuclear fuel. The ceramic waste form is prepared from hot isostatic pressing of a mixture of salt-occluded zeolite and glass binder. These composite materials were shown to be leach resistant (meeting standard criteria required for waste storage applications). While leach tests are generally satisfactory, however, some variability in performance has been observed.

Powder diffraction analysis of prospective zeolite waste form composites is important for correlating structural features with waste form capacity-controlling factors such as cation segregation, competition between charge balance and occlusion, mixed phase compositions and resistance to phase transformation during processing. This work has emphasized neutron diffraction for a number of reasons. Rietveld profile refinement of zeolite and molecular sieve structures using neutron powder diffraction data is well established [1-4]. In addition, the scattering contrast of important constituent elements in the composites is advantageous. These zeolite composites tend to exhibit strong long-range cation ordering. The strength of this ordering is evidenced by dramatic re-arrangement of oxygens in the zeolite framework to accommodate the long-range ordering. Oxygen is a relatively weak scatterer of X-rays, but an exceptionally strong scatterer of neutrons. Neutron diffraction patterns which are strongly influenced by oxygen scattering, therefore, allow us to follow in detail the accommodation of oxygen to waste salt occlusion. Furthermore, the scattering strength of Li is considerable with neutron diffraction, allowing us to recognize the strong impact Li has on the resulting structures.

Zeolites are very complex materials, even in their simplest chemical forms. Occlusion of simulated waste salts further complicates the structures, by producing strong distortions in  $AlO_4$  and  $SiO_4$  tetrahedra in the zeolite. General statements can, however, be made regarding the relationship between overall composition and resulting structure. This is because cations from the salt (Li in particular) dominate interactions with the zeolite, to induce surprisingly regular long-range structures. Salt-occluded zeolites with relatively high mass fractions of Li ( $\geq 4$  wt%) crystallize in a single phase structure with nearly absolute long-range ordering of cations, largely on the basis of size [5]. As will be discussed in this paper, mixtures prepared from zeolite 4A (with exclusively  $Na^+$  cations) and from zeolite 5A (roughly 60%  $Ca^{2+}$ , 40%  $Na^+$ ) also have structures

involving strong interactions between occluded salt complexes and the zeolite framework, but with different cation ordering schemes.

As part of the waste form processing, salt-occluded zeolites are pressure-bonded with borosilicate glass at an elevated temperature to form the final product. Under many circumstances, this high-temperature processing results in transformation of zeolite-A to the more dense zeolite known as sodalite. The susceptibility of the occluded zeolite to this conversion depends on the starting material; samples prepared with zeolite 5A are less likely to convert. The structures of zeolite 4A and zeolite 5A mixtures have been determined in an effort to identify correlations between cation distribution, etc. and susceptibility to transformation.

## EXPERIMENTAL

Salt-occluded zeolite samples are prepared using one of three methods [6-8]: (1) ion exchange, (2) occlusion or (3) a combination of (1) and (2). In method (1), the zeolite is treated with an excess of salt, usually a factor of 10:1 salt:zeolite, and ion exchange predominates. The concentration of fission products in the salt-occluded zeolite is high, usually over 10 wt% and there is little Na, <1 wt%. Most charge compensating ions are Li and K. This type of salt-occluded zeolite is referred to as fully exchanged zeolite. In method (2), excess zeolite is treated with a minimum of salt, and salt occlusion predominates. Typically, there is about 4 times as much zeolite as salt. Thus, the concentration of fission products in the salt-occluded zeolite is about 20% of that in the salt, about 1-3 wt%. The Na concentration is high, typically around 12-13 wt%. This type of salt-occluded zeolite is referred to as blended zeolite. In method (3), both the ion exchange and the occlusion methods are combined. The zeolite is first treated with excess salt, as in an ion exchange process. The zeolite is fully exchanged but contains a significant amount of surface salt. This surface salt is sorbed into new zeolite using the occlusion or second method. The combination method leads to intermediate fission product and Na concentrations.

Shown in Table 1 are the chemical compositions of salt-occluded zeolites used in our neutron powder diffraction studies. These were chosen to be representative of each of the methods described above. Samples identified as BE-4 and BE-5 were prepared using method (1), 3023-E, 4A-Sr, 4A-Y, 5A-Sr and 5A-Y were prepared using method (2), and 12223-D was prepared using method (3).

Table 1. Chemical compositions (wt%) for some of the salt-occluded zeolites studied

Ion	BE-4	BE-5	12223-D	3023-E	4A-Sr	4A-Y	5A-Sr	5A-Y
Li <sup>+</sup>	4.00	4.00	1.29	1.72	1.14	1.30	1.25	1.22
Y <sup>3+</sup>	0.46	1.34	0.01	0.00		1.52		3.01
Na <sup>+</sup>	0.60	0.60	7.04	11.20	12.80	13.00	3.49	3.83
Ca <sup>2+</sup>							7.66	7.45
Sr <sup>2+</sup>	3.45	1.71	0.06	0.61			3.24	
Ba <sup>2+</sup>	2.56	3.49	0.19	0.48				
K <sup>+</sup>	6.00	6.00	14.60	5.15	4.45	5.00	4.79	4.70
Cs <sup>+</sup>	7.75	8.02	0.67	1.38				
Cl <sup>-</sup>	16.00	16.00	12.60	12.60	11.30	12.00		

Salt-occluded zeolite samples, prepared as loose powders, were transferred to vanadium sample tubes and placed in the General Purpose Powder Diffractometer (GPPD) [9] at the Intense Pulsed Neutron Source (IPNS) at Argonne National Laboratory. Data collection times were in the range of 12 to 24 hours. Time-of-flight (TOF) neutron diffraction data (Figure 1) are accumulated at a series of fixed scattering angles on the GPPD, in the form of neutron counts as a function of interplanar d-spacings. Data from the highest resolution detectors ( $2\theta = \pm 148^\circ$ ) were analyzed using the Rietveld profile refinement technique [10] modified for TOF data [11]. As will be discussed in the following section, some occluded zeolite samples are single phase, while others are multi-phase.

Rietveld profile refinement provides an identification of space group and unit cell lattice parameters for each phase, along with a quantification of framework distortions and cation and

anion site positions and occupancies. Because most populated sites are of relatively high symmetry, far fewer refineable parameters are required to define the structures than the number of distinct diffraction data points (Bragg peak intensities).

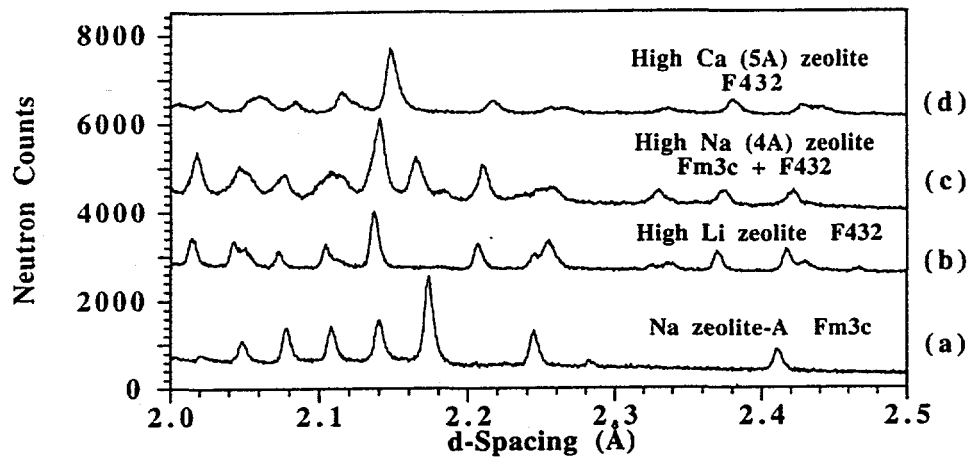


Figure 1. Comparisons of small sections of neutron diffraction patterns of Na zeolite-A and salt-occluded zeolite-A mixtures. These data show that: (a) Na zeolite-A is a simple fcc cubic phase, (b) compositions with high Li content are single phase with a more complex fcc cubic phases, (c) high Na mixtures are two phase; one phase similar to (a) and the other similar to (b), and (d) high Ca mixtures are single phase with a complex fcc cubic phase subtly different than (b). Note that in addition to the introduction of superlattice reflections, occlusion typically contracts the overall lattice, thus shifting reflections to lower d-spacings.

## RESULTS

### Description of zeolite-A and sodalite structures

The structures of zeolite-A and sodalite are well known, described by numerous crystallographic studies over the past few decades [12-14, and many more]. Both zeolite-A and sodalite are framework structures composed of  $\text{SiO}_4$  and  $\text{AlO}_4$  tetrahedra linked on corners to form micropores, and contain, as "building units", what are known as sodalite units (see Figure 2). In zeolite-A, isolated sodalite units, referred to as  $\beta$ -cages, are joined through linkages which have the appearance of cubes. Each "cube link" joins two  $\beta$ -cages. Sodalite appears to be assembled by the fusing of sodalite units into a structure made up entirely of sodalite units. A more appropriate description, though, would be to say that the sodalite structure is composed of sodalite units linked at edges, such that the linkages, themselves, are sodalite units. In this representation, each "sodalite link" joins four sodalite units. This picture illustrates a possible mechanism by which zeolite-A can transform to sodalite. If all of the "cube" linkages in zeolite-A are broken, and the dissociated sodalite units re-arrange themselves appropriately, the sodalite structure is generated.

Zeolite-A contains two types of micropores, large  $\alpha$ -cages bounded by 4-, 6- and 8-rings, and smaller  $\beta$ -cages bounded by 4- and 6-rings. For reference, a 6-ring, which is designated 6R, is a ring of atoms containing 6 oxygens, 3 silicons, and 3 aluminums (shown as hexagons in Figure 2). Synthetic Na zeolite-A has  $\text{Na}^+$  ions sitting in the large  $\alpha$ -cages opposite 6-rings (on 6R sites), off-center in 8-rings, and occasionally on 4R sites. The natural form of sodalite [14] has composition  $(\text{Na}_4\text{Cl})_2(\text{AlSiO}_4)_6$ , where chloride ions sit in the centers of sodalite units and sodium ions are on 6R sites, bridging the chloride ion and oxygens in the framework.

### Ion-exchanged zeolite-A

In zeolite-A, each  $\text{AlSiO}_4$  formula unit has a net charge of -1, corresponding to a total charge of -12 for each  $\alpha$ -cage. This negative charge must be balanced by extra-framework cations. In Na

zeolite-A, this is accomplished with  $\text{Na}^+$  ions on 6R, 8R and 4R sites [15]. In cation exchanged forms of zeolite-A, the siting of cations is often more complex [16-20]. Diffraction studies have described the behavior of virtually all of the cations considered here, when they are present alone as ion-exchanged species. In all cases, 6R sites are the most highly populated.  $\text{Li}^+$  ions in Li-exchanged zeolite-A (Li-A) are positioned off center in the 6-rings, producing a long range distortion of the framework [work in progress]. In the  $\text{K}^+$  [16],  $\text{Ca}^{2+}$  [17] and  $\text{Sr}^{2+}$  [18] forms, some 6R ions project into the smaller  $\beta$ -cages. Partially exchanged Cs-A has  $\text{Cs}^+$  ions on 6R sites in  $\alpha$ - and  $\beta$ -cages and on 8R and 4R sites, with  $\text{Na}^+$  ions on 6R sites in  $\alpha$ -cages [19]. Commercial 5A zeolites (with  $\text{Ca}^{2+}:\text{Na}^+ = 5:2$ ), have  $\text{Ca}^{2+}$  ions in  $\beta$ -cages on 6R sites and  $\text{Na}^+$  ions on 6R sites in  $\alpha$ -cages [2].

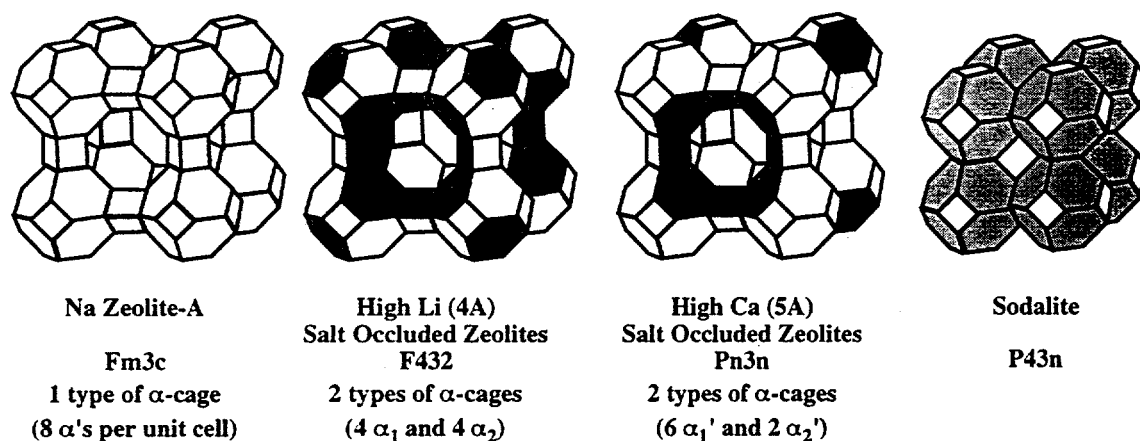


Figure 2. Structural drawings of zeolite-A and sodalite. The vertices of line segments correspond, alternately, to Si and Al atoms, and the mid-point of each line represents an O atom. Zeolite-A is composed of sodalite units ( $\beta$ -cages) joined by "cube linkages", while sodalite is composed of sodalite units joined by "sodalite linkages" (see text for details). Shading of the  $\alpha$ -cage surfaces refers to the type of cation clusters present, i.e., predominately Li-K-Cl vs. predominately fission product-Cl.

### Salt-occluded zeolites

As described above, salt-occluded zeolites are prepared using a variety of methods. Neutron diffraction studies have shown that the resulting structures (siting of cations) depend both on the method of preparation, and the overall composition of the salt solution used in the preparation. To illustrate this point, the following paragraphs will highlight the characteristics of sample compositions shown in Table 1.

Salt-occluded zeolites prepared using the ion exchange method, which result in mixtures with Li compositions higher than 3 wt%, have a strongly long-range ordered structure [5]. Figure 1 provides direct evidence of the long-range ordering, namely additional superlattice diffraction lines in the neutron diffraction patterns. This ordering is found to be due to the presence of two types of  $\alpha$ -cages,  $\alpha_1$  with predominately  $\text{Li}^+$  on 6R and 4R sites and  $\text{K}^+$  on 8R sites, and  $\alpha_2$  with predominately large fission product ions ( $\text{Cs}^+$  and  $\text{Ba}^{2+}$ ) on 6R sites. The "NaCl-like" ordering of  $\alpha$ -cages, whereby  $\alpha$ -cages sharing 8-rings are different (i.e., neighboring cages have different colors or shading), is schematically illustrated in Figure 2. The long-range ordering is propagated by very strong distortions of the  $\text{AlSiO}_4$  framework generated in order for  $\text{Li}^+$ , with its high charge-to-radius ratio, to closely bond with oxygens in the zeolite. In this model,  $\text{Li}^+$  in  $\alpha_1$ -cages and  $\text{Cs}^+$  and  $\text{Ba}^{2+}$  in  $\alpha_2$ -cages, in addition to playing the charge balancing role described above, are inter-linked within  $\alpha$ -cages through bonds with  $\text{Cl}^-$  ions. Finally, in the  $\alpha_2$ -cages, on average only half of the 6R sites are populated by  $\text{Cs}^+$  or  $\text{Ba}^{2+}$ . The remaining 6R sites were found to be

populated by  $\text{Sr}^{2+}$ ,  $\text{Y}^{3+}$  (smaller fission product ions) and  $\text{Li}^+$ , where the ions project into the smaller  $\beta$ -cages.

Salt-occluded zeolites prepared with Na zeolite-A are two phase mixtures. While it is not readily apparent in Figure 1, where peaks from the two phase are strongly overlapped, Rietveld refinements revealed that two phases are present, and they are qualitatively similar to Na zeolite-A and high Li salt-occluded zeolite, respectively. Although refinements are relatively qualitative, Li-dominated ordering persists in the primary occluded zeolite. In the "Na zeolite-A" phase, in addition to  $\text{Na}^+$  and, seemingly, some fission product ions occupying traditional 6R and 8R sites,  $\text{Cl}^-$  ions link cations in a similar manner to that observed in the high Li zeolites, without producing a superlattice, i.e., there is only one type of  $\alpha$ -cage.

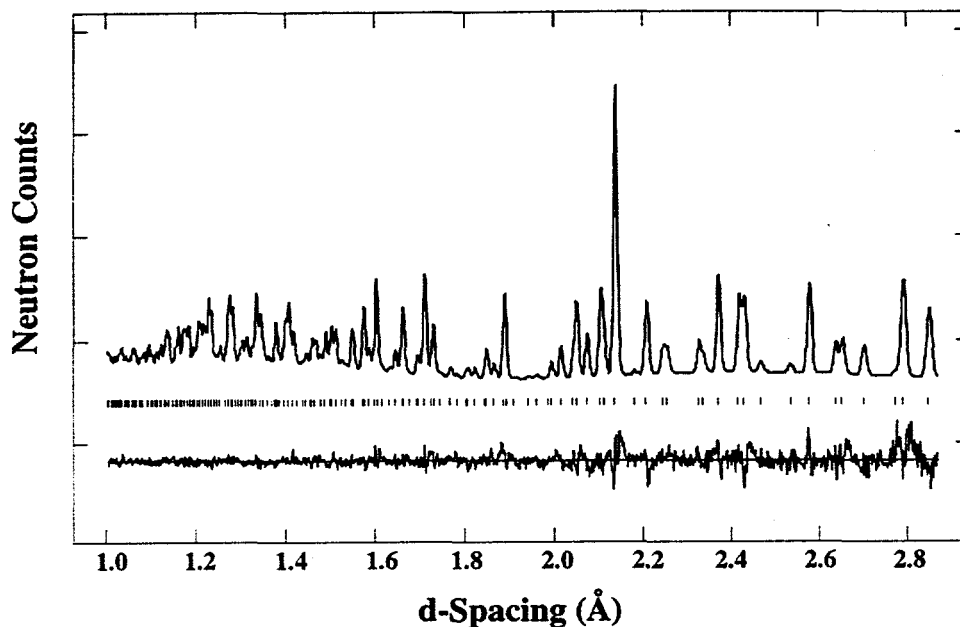


Figure 3. Rietveld profile refinement plot, showing fit to the neutron diffraction pattern of a salt-occluded zeolite, designated Sr-5A, prepared with the occlusion method using zeolite 5A (60% Ca, 40% Na) as starting material. The data points are observed data, the smooth curve through the data is the calculated diffraction spectrum, the residual (obs - calc) is shown at the bottom, and the vertical bars identify d-spacings for reflections.

Samples prepared using the occlusion method with zeolite 5A ( $\text{Ca}^{2+}$  and  $\text{Na}^+$  as charge compensating cations) as starting material have a slightly different structure than those prepared from Na zeolite-A. These samples have single phase, long-range ordered structures, similar to the high Li zeolites. But the ordering pattern is slightly different. Rather than the "NaCl-like" behavior found in Li-rich occluded zeolites, the ordering is more reminiscent of "Cu<sub>3</sub>Au-like" ordering in simple intermetallic alloys. Whereas in the "NaCl-like" ordering, 4 out of 8  $\alpha$ -cages per unit cell are of  $\alpha_1$  type and the other 4 of  $\alpha_2$  type, according to this ordering pattern, 6 out of 8  $\alpha$ -cages per unit cell are  $\alpha_1'$ , and the other 2 are  $\alpha_2'$ . Rietveld refinements (see Figure 3 for the profile fit) suggest that in the  $\alpha_1'$ -cages,  $\text{Li}^+$  and  $\text{K}^+$  ions occupy 6R sites, with  $\text{Cl}^-$  ions linking cations, while the fission products occupy 6R sites in the  $\alpha_2'$ -cages, again with  $\text{Cl}^-$  linkages. The fundamentally different feature in these occluded zeolites is the presence of large amounts of  $\text{Ca}^{2+}$  ions in  $\beta$ -cages, opposite 6R sites occupied by  $\text{K}^+$ .

#### Resistance to sodalite transformation

The postulated mechanism for the transformation of salt-occluded zeolite to sodalite requires that Al-O and Si-O bonds in the linkages between  $\beta$ -cages become de-stabilized. This de-stabilization is probably a consequence of many factors, but must have some relationship to the fre-

quency and type of interactions between the critical oxygens (those whose bonds must be broken) and occluded cations. We have learned from these neutron diffraction analyses that, in Ca-rich salt-occluded zeolites, many  $\text{Ca}^{2+}$  ions remain in  $\beta$ -cages (i.e.,  $\text{Ca}^{2+}$  is less readily exchanged than  $\text{Na}^+$ ), and that the long-range ordering sequence is different from that of Na-rich occluded zeolites. The degree of de-stabilization is anticipated, then, to be strongly related to the degree of long-range ordering exhibited by the  $\beta$ -cage occluded  $\text{Ca}^{2+}$  ions.

## CONCLUSIONS

Time-of-flight neutron diffraction data from IPNS have provided detailed crystallographic information on the sites and populations of occluded simulated waste ions in salt-occluded zeolites. The unexpected level of detail observed is largely due to the tremendous flexibility of the zeolite-A framework, and its capacity to promote ordering of cations over large length scales. The discovery of strong crystallographic ordering in chloride salt-occluded zeolite-A mixtures may be important when postulating cation migration and transmutation during long-term storage. Finally, it is not absolutely certain how the characteristic cation siting and long-range order interplay to influence the transformability of salt-occluded zeolites in the high temperature bonding environment. Our new understanding of these factors for a variety of compositions at ambient temperature and pressure, though, will be extremely valuable for future studies of these materials under conditions simulating the bonding operation.

## ACKNOWLEDGMENTS

The submitted manuscript has been authored by contractors of the U.S. Department of Energy (BES-Materials Sciences) under contract No. W-31-109-ENG-38. Accordingly, the U.S. Government retains a non-exclusive royalty-free license to publish or reproduce the published form of this contribution, or allow others to do so, for U.S. Government purposes.

## REFERENCES

1. J. M. Adams and D. A. Haselden, *J. Solid State Chem.* **47**, 123 (1983).
2. J. M. Adams and D. A. Haselden, *J. Solid State Chem.* **51**, 83 (1984).
3. J. W. Richardson, Jr., J. V. Smith and J. J. Pluth, *J. Phys. Chem.* **93**, 8212 (1989).
4. J. W. Richardson, Jr. and E. T. C. Vogt, *Zeolites* **12**, 13 (1992).
5. J.W. Richardson, Jr., M. A. Lewis and B. R. McCart, *Proc. 10th Int. Zeol. Conf.* 741 (1994).
6. M. A. Lewis, L. J. Smith and D. F. Fischer, *Am. Ceram. Soc.* **11**, 2826 (1993).
7. M. A. Lewis, D. F. Fischer and C. D. Murphy, *Mat. Reser. Soc. Proc.* **333**, 277 (1994).
8. M. A. Lewis, D. F. Fischer and C. D. Murphy in *Environmental and Waste Management Issues in the Ceramic Industry II*, 277 (1994).
9. J. D. Jorgensen, J. Faber, Jr., J. M. Carpenter, R. K. Crawford, J. R. Hauman, R. L. Hitterman, R. Kleb, G.E. Ostrowski, F.J. Rotella and T.G. Worlton, *J. Appl. Cryst.* **21**, 321 (1989).
10. H. M. Rietveld, *J. Appl. Cryst.* **2**, 65 (1969).
11. A. C. Larson and R. B. Von Dreele, GSAS, General Structure Analysis System. Los Alamos National Laboratory Report LAUR86-748 (1986).
12. T. B. Reed and D. W. Breck, *J. Am. Chem. Soc.* **78** (1956) 5972.
13. V. Gramlich and W. M. Meier, *Z. Krist.* **133**, 134 (1971).
14. L. Pauling, *Z. Krist.* **74**, 213 (1930).
15. J. J. Pluth and J. V. Smith, *J. Am. Chem. Soc.* **102**, 4704 (1980).
16. J. J. Pluth and J. V. Smith, *J. Phys. Chem.* **83**, 741 (1979).
17. J. J. Pluth and J. V. Smith, *J. Am. Chem. Soc.* **105**, 2621 (1983).
18. J. J. Pluth and J. V. Smith, *J. Am. Chem. Soc.* **104**, 6977 (1982).
19. N. H. Heo and K. Seff, *J. Am. Chem. Soc.* **109**, 7986 (1987).
20. J. M. Newsam, R. H. Jarman and A. J. Jacobson, *J. Solid State Chem.* **58**, 325 (1985).